RESEARCH

Assessment of the petrophysical properties and hydrocarbon potential of the Lower Miocene Nukhul Formation in the Abu Rudeis-Sidri Field, Gulf of Suez Basin, Egypt

Sherif Farouk · Souvik Sen · Nancy Belal · Mohammad A. Omran · Ehab M. Assal · Mohammad A. Sarhan

Abstract Lower Miocene rift sediments of the Nukhul Formation are one of the prominent hydrocarbon producers in the Gulf of Suez basin. In this study, we focused on the oil producing Nukhul sandstones of the Abu Rudeis-Sidri Field, located in the east central Gulf of Suez. Nukhul Formation is characterized by the prominent low amplitude seismic reflectors and represents the youngest identified reflector (Lower Miocene) in the study area. Petrophysical assessment was carried out using wireline logs to infer the reservoir characteristics. The Nukhul sandstone reservoir exhibits lower shale volume (<0.1 dec dominantly), 0.07–0.16 dec total porosity and effective porosity up to 0.13 dec within the Nukhul sandstone interval. Bulk density-neutron porosity cross plot infers primarily sandstone matrix with the influence of carbonates, which characterizes the studied reservoir as calcareous sandstones. Spectral gamma ray data indicates montmorillonite as the principal clay phase along with minor kaolinite and illite. The calculated water saturation of the reservoir zone in the three productive wells ranges between 0.17 and 0.34 dec (i.e., the hydrocarbon saturation equals 0.66–0.87 dec). A small range of bulk volume of water (0.011–0.03 dec) indicates superior quality of the hydrocarbon-bearing sandstone intervals. Absence of productive sands in one of the studied wells, drilled in the hanging wall implied structural control on hydrocarbon accumulation in the study area. This study provides crucial insights regarding the quantitative petrophysical characteristics, reservoir quality distribution and hydrocarbon potential of the Lower Miocene Nukhul clastic reservoir.

Highlights

- This study presents the quantitative petrophysical characterization of the Lower Miocene Nukhul sandstones.
- The reservoir sandstones are calcareous in nature and consist of montmorillonite as the dominant clay phase.
- Reservoir exhibits very high hydrocarbon saturation with high lateral variations in porosity and shale volume.

S. Farouk
Exploration Department, Egyptian Petroleum Research Institute (EPRI), 1 Ahmed El-Zomor Street, Nasr City 11727, Cairo, Egypt

S. Sen
Geologix Limited, Andheri (E), Mumbai, Maharashtra 400059, India

Present Address:
S. Sen
Halliburton Consulting, Mumbai, India

N. Belal · M. A. Omran · E. M. Assal · M. A. Sarhan (✉)
Geology Department, Faculty of Science, Damietta University, New Damietta City, Damietta 34517, Egypt
e-mail: msarhan@du.edu.eg

Abbreviations

GR	Gamma ray log (API)
GRmin	Minimum gamma ray value of an interval (API)
GRmax	Maximum gamma ray value of an interval (API)
Vsh	Shale volume (decimal)
Sw	Water saturation (decimal)
BVW	Bulk volume of water (decimal)
Rsh	Shale resistivity (Ωm)
Rt	Deep resistivity log (Ωm)
Rw	Resistivity of the connate water (Ωm)
a	Tortuosity factor (–)
m	Cementation exponent (–)
n	Saturation exponents (–)
Φt	Total porosity (decimal)
Φe	Effective porosity (decimal)
Φnphi	Neutron porosity (decimal)
Φρb	Density porosity (decimal)

1 Introduction

The Gulf of Suez region is the most productive oil rift basin in Africa and the Middle East, and it contains more than 80 active oil fields (Schlumberger 1995; Alsharhan 2003; El Nady et al. 2015; Moustafa and Khalil 2020; Kassem et al. 2021; Radwan and Sen 2021a, b, c, d; Radwan 2021a, b). Many studies on the evolution of the Gulf of Suez rift have been conducted, including structural and sedimentological studies due to the well-exposed syn-rift formations and the large amounts of exploration data on this region (Winn et al. 2001; Radwan et al. 2020, 2021a, b, c). The fault blocks that started at the rifting period represent the main hydrocarbon traps and rule the petroleum accumulation in the Gulf of Suez oil fields (Chowdhary and Taha 1987; Sultan 2002). The Miocene successions in the Gulf of Suez have attracted the attention of many geologists due to their economic importance for oil and gas. The Lower and Middle Miocene Syn-rift sediments are the most prolific petroleum reservoirs in the Suez province. During the early evolution of the Gulf of Suez and Red Sea Syn-Rift System, the Lower Miocene of Egypt (Nukhul Formation) was deposited and it's the oldest and most overall Syn-rift sediments in the Gulf of Suez (Al-Husseini 2012). In more than 15 fields, the Nukhul Formation is a high-quality petroleum reservoir (Saoudi and Khalil 1986). Nukhul is oil producing in Rudeis-Sidri, Zeit Bay, Hilal, GS173, Darag and Ashrafi fields, while it produces both oil and gas in the Hareed field (Alsharhan 2003). Overall, it contributes to roughly 11.5% of production potential of Gulf of Suez (Alsharhan 2003).

This study focuses on the Abu Rudeis-Sidri Field from Gulf of Suez (Fig. 1). The field produces an average of 2700 BOPD, mostly from Nukhul Formation, with least amounts from the Thebes, Matulla and Nubia intervals (Fahmi et al. 2015). Zahra and Nakhla (2016a, b) inferred the structural settings of the northeastern Gulf of Suez area including Rudeis-Sidri field, using aeromagnetic and seismic data. Burial history and thermal evolution of the field was inferred by Awadalla et al. (2018). Organic-rich pre-Miocene Thebes Formation is the prominent source rock in the Abu Rudeis-Sidri field (Mostafa and Ganz 1990; Mostafa et al. 1993; Awadalla et al. 2022). Elmaadawy et al. (2021) characterized the source rock characteristics of the Duwi and Thebes intervals in the study area. A few researchers worked on the new unconventional reservoir characteristics and potential of the Oligocene–Miocene fractured igneous intrusions (Fahmi et al. 2015; Abd-El Gawad et al. 2022). Till date, the petrophysical properties of the Nukhul producers have not been published, which sets the premise of this work. Wireline log-based quantitative petrophysical interpretation is critical for inferring reservoir pay zone and its production potential which has direct implications for field development planning and resource optimization (Haque et al. 2022). Reservoir characterization quantifies physical and fluid properties of rocks such as porosity, shale volume, fluid saturation (Islam et al. 2021; Qadri et al. 2022; Zhang et al. 2022) and to be integrated with geological, geophysical, structural inferences and basin analysis approaches to get a clear subsurface understanding of the subsurface reservoir distribution (Cheng et al. 2014; Adelu et al. 2019; Jenkins and Torvela 2020). The main aim of this study was to assess the key petrophysical properties of the Nukhul Formation in the Abu Rudeis-Sidri Field, which includes volume of shale, total and effective porosities, water saturation and bulk volume of water.
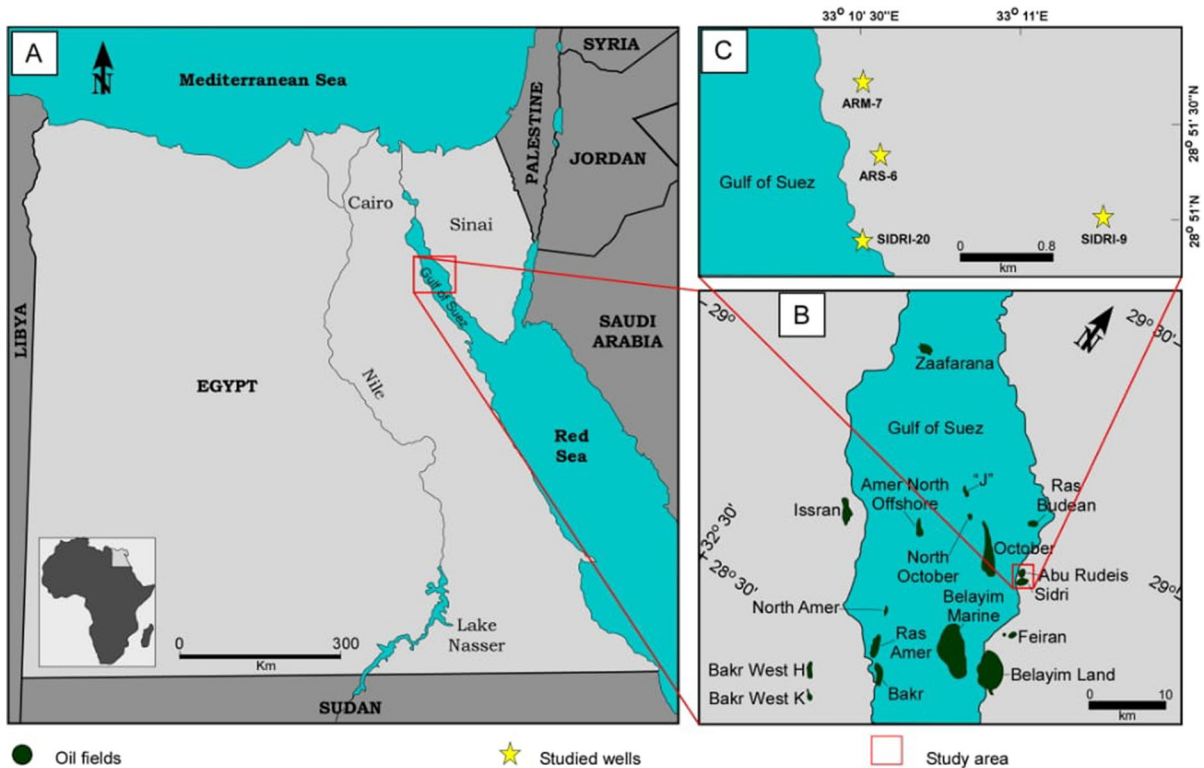
Fig. 1 **A** Location map of the study area in Egypt; **B** location of the studied Abu Rudeis-Sidri field in the Eastern part of the Gulf of Suez, modified after Youssef (2011); **C** location of the four studied wells

Wireline logs have been the primary input parameter for the petrophysical analysis. Inferences have been drawn on lithological characteristics and clay mineralogy. Focused characterization and reevaluations of the already discovered petroleum systems and producing reservoirs are required to assess the reservoir's ability and potential to meet the economic and field development requirements (Zhang et al. 2022). Our study is focused on that aspect of the Nukhul Formation from the Abu Rudeis-Sidri field. The quantitative petrophysical assessment presented in this study sheds critical insight about the reservoir quality of the Nukhul sandstones, provides high reliability about its hydrocarbon potential and thereby reducing the risks associated with hydrocarbon exploration.

2 Geological setting

The rifting of the Gulf of Suez started during the Lower Miocene due to the divergent movement between the African plate and the Arabian plate which created a series of NW–SE to NNW–SSE trending normal faults (Patton et al. 1994; Omran 1995; Abul Karamat and Meshref 2002; Bosworth et al. 2005). The faulted blocks of the Gulf of Suez are bounded mainly by NW normal faults and connected to each other by WNW-, NNE- and NE-oriented faults (Abd-Allah et al. 2014). The syn-rift Miocene deposit in the Gulf of Suez province changes laterally from clastic sediments to more deeply buried sediments towards the rift axis (Bosworth and McClay 2001). Due to the tilt of the pre-rift blocks, the Miocene rocks overlying the different pre-rift units vary in lithologies and thicknesses (Abd-Allah et al. 2014). The structure of Abu Rudeis-Sidri area is an asymmetrical NW–SE trending anticlinal feature separated by a number of NW–SE fault systems and formed during the late Oligocene-Early Miocene time (rifting phase) (Zahra and Nakhla 2016b). A stratigraphic chart is presented in (Fig. 2) which reflects the change in depositional environment (continental to shallow/
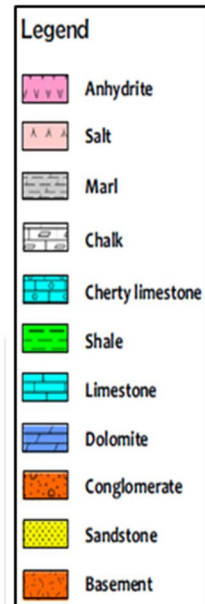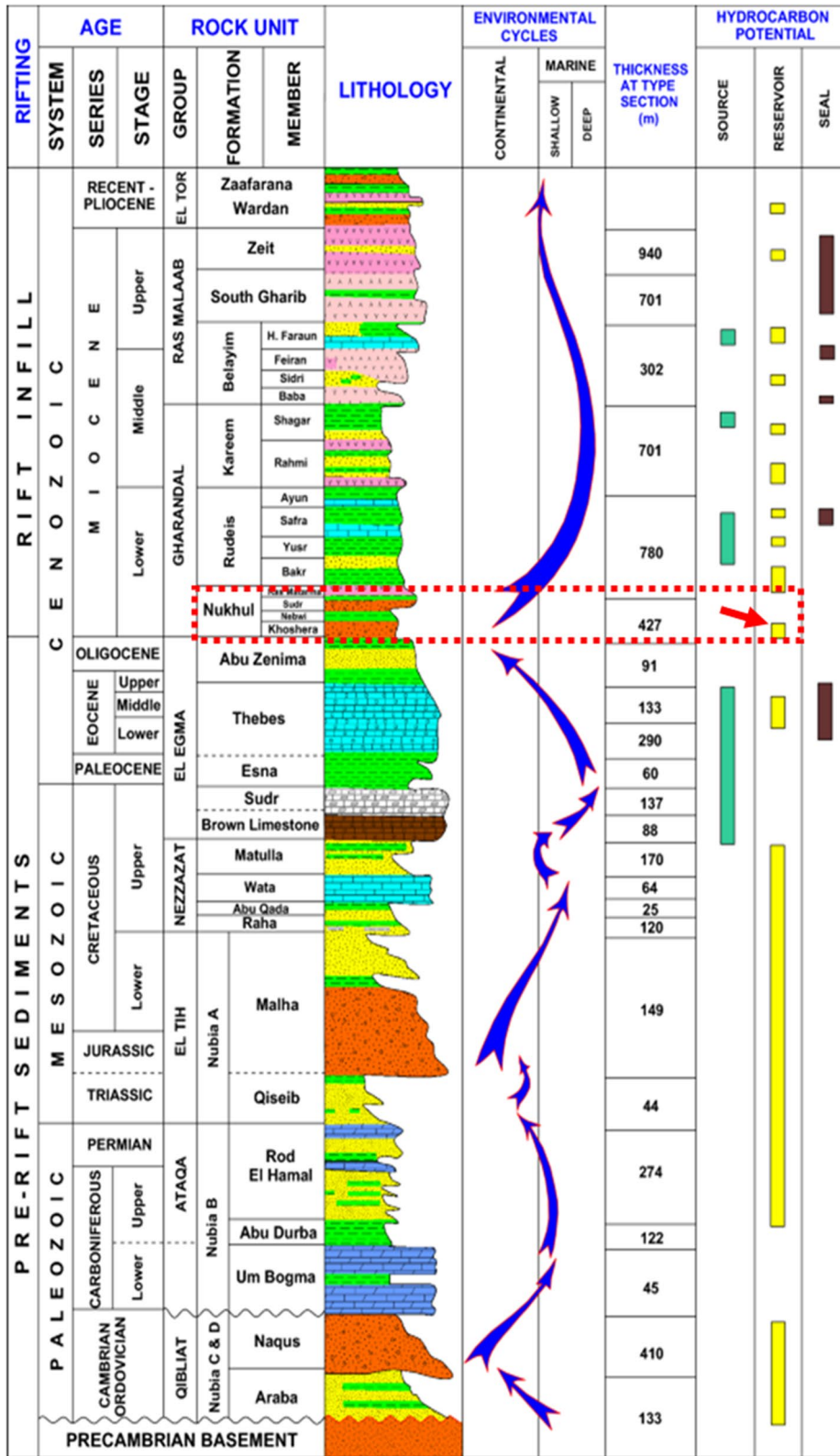
◄**Fig. 2** General stratigraphic chart of the Gulf of Suez Basin, after El Diasty et al. (2020)

deep marine) with geological time (refer to the arrows in Fig. 2), in relation to sea level fluctuations (El Diasty et al. 2020). The lower-middle Miocene succession in the Abu Rudeis-Sidri Field includes the Kareem, Rudeis, and Nukhul formations from top to bottom. Nukhul Formation unconformably lies above the Oligocene Abu Zenima Formation (mostly conglomerate) and conformably overlain by Rudeis Formation. The Nukhul Formation was first described by (Waite and Pooley 1953) as the basal marine Miocene beds in Sinai and Gulf of Suez regions and first introduced by (Ghorab 1964) in a type-section, south of Wadi Nukhul area (29º 01′ N, 33º 11′ E). In the subsurface succession, The Nukhul Formation was introduced by the National Stratigraphic Subcommittee of the Geological Sciences of Egypt (NCGS 1974). According to (Schutz 1994; Abd El Gawad et al. 2016), the Nukhul interval was deposited in a shallow marine condition. Generally, the Nukhul Formation in Abu Rudeis-Sidri Field consists of shale interbedded with few limestones and sandstones. It has a relatively small thickness in outcrops, but borehole data indicates a large thickness up to 500 m in the West Zeit trough (Peijs et al. 2012). Saoudi and Khalil (1986) reported that Nukhul Formation in Wadi Nukhul consists only of 60 m thick.

3 Materials and methods

In this study, we have analyzed four drilled wells: ARS-6 (latitude 28° 51′ 20.23″ N, longitude 33° 10′ 33.52″ E), ARM-7 (latitude 28° 51′ 43.05″ N, longitude 33° 10′ 30.36″ E), Sidri-9 (latitude 28° 51′ 0.7″ N, longitude 33° 11′ 15.23″ E), and Sidri-20 (latitude 28° 50′ 53.42″ N, longitude 33° 10′ 28.24″ E) (Fig. 3).

3.1 Well logging

Wireline logs were available from all the four wells which include gamma ray, formation resistivity, neutron porosity and bulk-density. Spectral gamma ray log was available from the well Sidri-9 which provided Uranium, Thorium and Potassium concentrations. All the wells had log data coverage within the

Nukhul Formation which is the main target interval for this work. Density log was checked for possible low value responses due to wash out conditions, but caliper log indicated gauged wellbore confirming data quality unaffected by borehole conditions. Mudlogs were also available from all the wells which provided drilling cutting lithological descriptions and used as primary lithology indicators.

3.2 Seismic data interpretation

In this study, we briefly looked into the seismic dataset to understand the lateral distribution of the stratigraphic units across various fault blocks. Seismic reflection profiles provide different fault dips and subsurface structural trends (Khan et al. 2021). Seismic interpretation involves the correlation between seismic data and available well logs (i.e., well tie) to identify consistent stratigraphic sequences and therefore establish the relationship between the stratigraphy and their corresponding seismic reflections (Qadri et al. 2017). Since the primary objective of this study was to assess the key reservoir petrophysical properties, a detailed seismic interpretation was out of scope. Eighteen seismic sections were available from the study area which was tied to four drilled wells. We presented the interpretation of three seismic lines (seismic line No. 89-19-GL-83-05-N, line No. 98-19-GJ-83-07-N and line No. RS-14-83-mig 160001) in this study. The horizons were marked on each seismic dip/strike cross-section by differentiating marker strata and other corresponding points assigned to well logs with primary reflections on the seismic cross-section. The various formation reflectors were identified according to their seismic characters. The continuity, geometry and reflector spacing were used to identify these reflectors. Seismic reflector on the top of the target formation, i.e., Nukhul Formation was picked and marked on the seismic sections along and faults were picked.

3.3 Petrophysical analysis

We analyzed these well logs to identify the hydrocarbon bearing zones within Nukhul Formation to perform the log-based petrophysical analysis. Lithology was interpreted from neutron porosity-bulk density cross plot and clay mineralogy was inferred from Thorium and Potassium concentration available from

Fig. 3 Seismic lines and location of the four studied wells within Abu Rudeis-Sidri Field (Figs. 5, 6 marked in red)
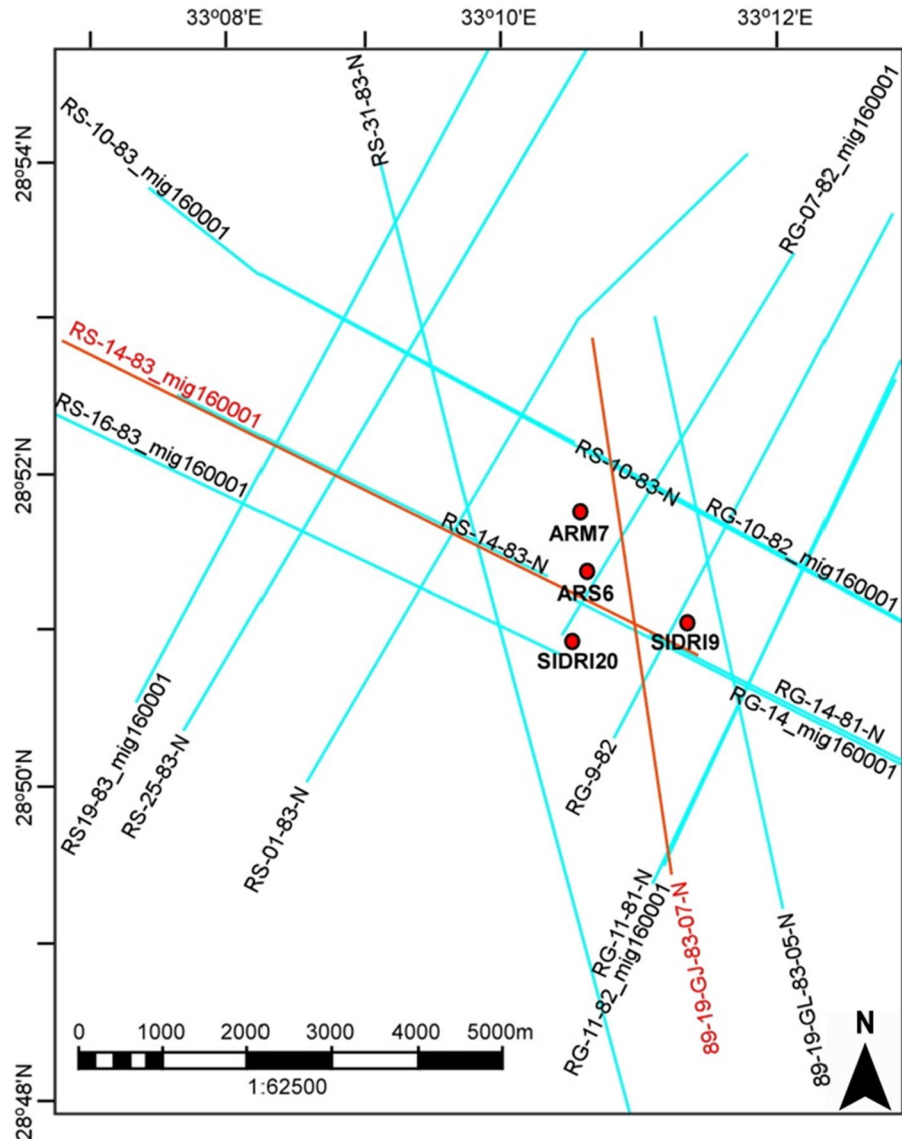
the spectral gamma ray data (Qadri et al. 2019). Five key petrophysical parameters were estimated from well logs: shale volume, (Vsh) total porosity (Φt), effective porosity (Φe), water saturation (Sw) and bulk volume of water (BVW).

Shale volume was estimated using gamma ray (GR) log (Asquith and Gibson 1982):

$$Vsh = \frac{GR - GRmin}{GRmax - GRmin} \tag{1}$$

where GRmin and GRmax denote the minimum and maximum GR values of the interval of interest, respectively. Total porosity was estimated using

bulk-density and neutron porosity logs (Asquith and Gibson 1982):

$$\Phi t = \frac{\Phi nphi + \Phi\rho b}{2} \tag{2}$$

where $\Phi nphi$ and $\Phi\rho b$ represent neutron porosity and density porosity, respectively. $\Phi\rho b$ is dependent on matrix density and formation fluid density (Qadri et al. 2019). Effective porosity is influenced by shale volume, and it was estimated as (Asquith and Gibson 1982):

$$\Phi e = (1 - Vsh) * \Phi t \qquad (3)$$

Indonesian water saturation model was utilized to estimate Sw (Poupon and Leveaux 1971):

$$Sw = \left\{ \frac{\sqrt{\frac{1}{Rt}}}{\left\{ \left(\frac{Vsh^{1-0.5Vsh}}{\sqrt{Rsh}} \right) + \sqrt{\frac{\Phi e^m}{aRw}} \right\}} \right\}^{\frac{2}{n}} \qquad (4)$$

where Rsh = shale resistivity, Rt = deep resistivity log, Rw = resistivity of the connate water, a = tortuosity factor, m = cementation exponent, n = saturation exponents, respectively. For the studied Nukhul Formation, we have considered Rw as 0.03 Ωm, a = 1, m = n = 2. A 50% water saturation cut off was utilized to distinguish between water wet and hydrocarbon bearing intervals (Qadri et al. 2019). Bulk volume of water (BVW) in uninvaded zone was estimated from Φe and Sw, following Buckles (1965):

$$BVW = \Phi e * Sw \qquad (5)$$

Based on the petrophysical properties, productive reservoir zones are interpreted within the Nukhul Formation. Results are discussed and compared with the other producing Nukhul intervals from offset fields. Inferences are drawn based on the regional geological understanding.

4 Results

4.1 Seismic data interpretation

On seismic sections, three formation intervals are interpreted, Kareem, Rudeis and Nukhul formations from top to bottom (Fig. 4). Kareem Formation, above the Rudeis interval, is characterized by very high amplitude reflectors with parallel to sub parallel configurations and medium continuity. It is considered as a marker reflector in the study area. It is very easy to pick this horizon due to its strong appearance and its distinguished high amplitude characters (Fig. 4). Rudeis Formation lies between the Rudeis and Nukhul Formations. It is characterized by medium amplitude reflectors that shows sub-parallel

Fig. 4 Seismic cross section with well tops marked on Sidri-9 profile (seismic line No. 89-19-GL-83-05-N)
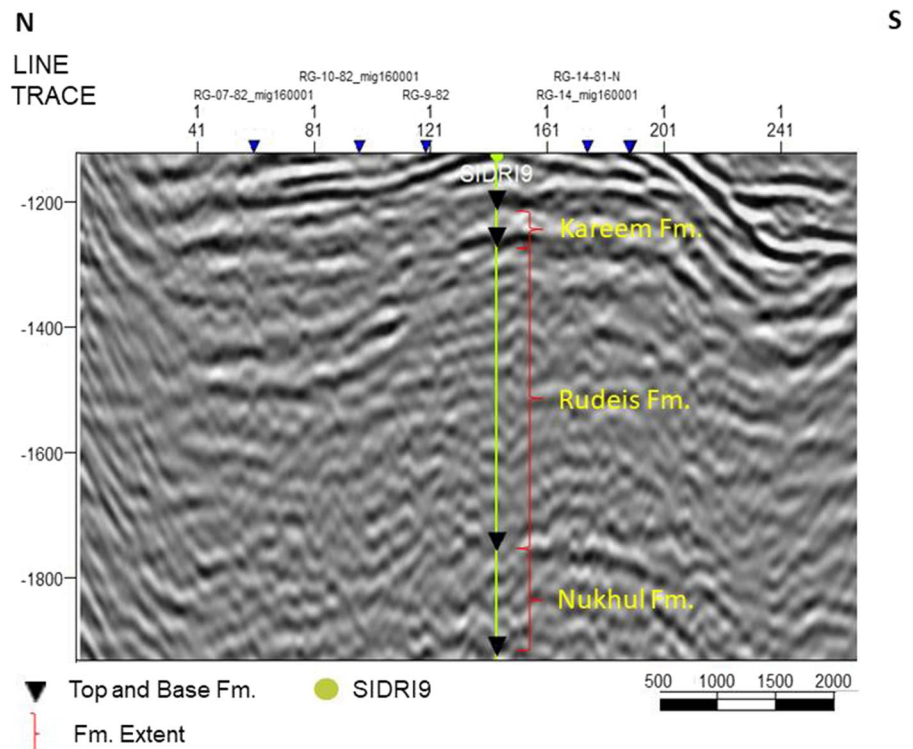
configurations at its base and high amplitude reflectors with parallel configurations at its top.

Nukhul Formation is the most prominent reflector in the Gulf of Suez. It represents the youngest identified reflector (Lower Miocene) characterized by low amplitude reflectors that exhibit sub-parallel configurations with low continuity due to the compressional forces affecting the area. Its low amplitude characteristics make it hard to pick the horizon. On seismic sections, the top of the Nukhul Formation is represented by a medium amplitude crinkled reflector intersected and cut by numerous steeply dipping normal faults, forming an extensional fault block (Figs. 5, 6). The occurrence of these normal faults is related to the opening of the Gulf of Suez during the Miocene reflecting the extensional regime.

4.2 Petrophysical interpretation

The Nukhul Formation has been characterized based on the wireline logs. We also integrated cuttings lithology from the available mud logs data. The Nukhul Formation consists of interbedded sandstone, shale, and limestone units. The top of Nukhul Formation is marked by a limestone interval. Quantitative petrophysical assessments of the Nukhul Formation in the studied wells are presented in Figs. 7, 10, 11 and 12. In the well ARS-6, the sandstone interval between 2809 and 2824 m exhibits low gamma ray, high resistivity, and density-neutron cross-over (Fig. 7). Cross plot between bulk-density and neutron porosity in the ARS-6 indicates sandstone matrix (Fig. 8), as also confirmed by the cutting lithology information (Fig. 8). The mentioned interval is characterized by $Vsh < 0.03$ dec (average value of 0.008 dec), $0.05 < \Phi t < 0.16$ (average value of 0.097 dec), $0.03 < \Phi e < 0.15$ (average value of 0.095 dec). Sw varies between 0.20 and 0.66 dec, while average Sw is observed as 0.33. In the Pickett plot (Pickett, 1972), the ARS-6 pay sand exhibits cluster around 25% Sw line which indicates good hydrocarbon potentiality (Fig. 9). Based on the estimated porosity and water saturation BVW is found to be 0.014–0.049 (average value of 0.03). In the well ARM-7, the equivalent sandstone interval occurs around 3383–3388 m, which lies just below the limestone intervals defining the top of Nukhul Formation. This sandstone interval has around 0.22 dec Vsh, Φt of 0.07 dec, Φe of 0.02 and Sw around 0.9, and inferred to be water-bearing and hence unproductive (Fig. 10).

In the Sidri-20 well, the productive sandstone interval is inferred between 2631 and 2646 m. The

Fig. 5 Interpreted seismic line No. 98-19-GJ-83-07-N (please refer to the Fig. 3 for the line position on the map)
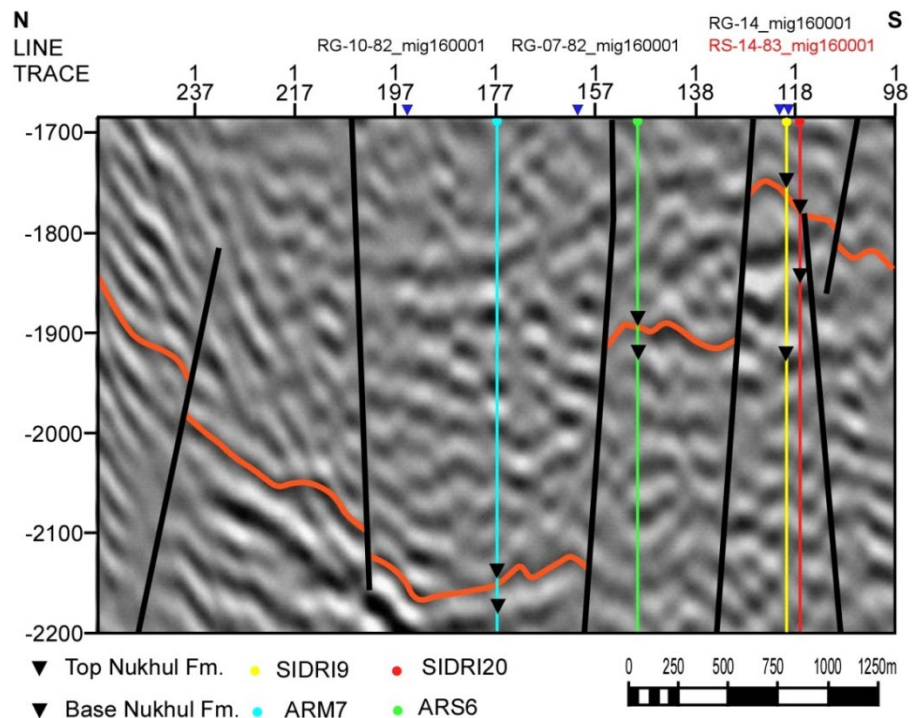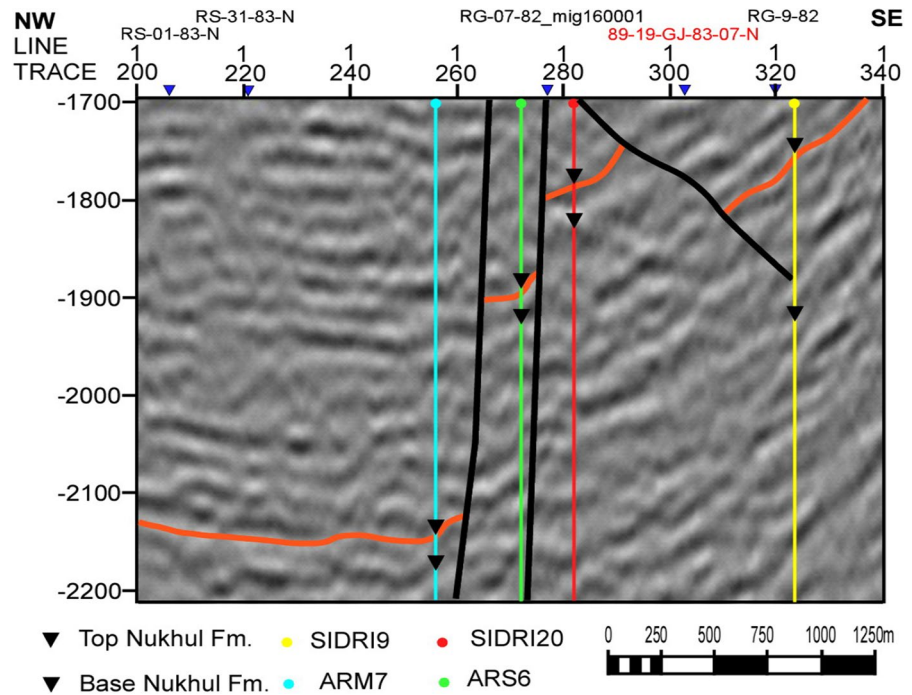
Fig. 6 Interpreted seismic line No. RS-14-83-mig 160001 (please refer to the Fig. 3 for the line position on the map)

zone is characterized by low gamma ray high resistivity and density-neutron cross-over (Fig. 11). Estimated Vsh varies between 0.07 and 0.41 dec with an average value of 0.25. Average porosities are observed to be less than 10% ($\Phi t \sim 0.07$ dec, $\Phi e \sim 0.04$ dec). Sw varies between 0.13 and 0.54 dec (average 0.33 dec) and average BVW is 0.011. Petrophysical analysis of the well Sidri-9 well is presented in Fig. 12. Like the other studied wells, Nukhul Formation top in Sidri-9 is also marked by a limestone interval. We inferred two pay sands in the Nukhul Formation between 2593–2612 and 2620–2628 m. Both the sands are characterized by low gamma ray (serrated signature), high resistivity and exhibit density-neutron cross-over. Both these sand intervals are separated by limestone parting (with minor shale). The upper sand is thicker and exhibits more porosity ($\Phi t \sim 0.16$ dec, $\Phi e \sim 0.13$ dec). Average Vsh is around 0.09, with ~ 0.30 dec Sw and 0.036 dec BVW (Fig. 12). In comparison with the upper reservoir, the lower one is thinner but observed to be cleaner with average Vsh of 0.03. Based on the neutron and bulk-density data, the lower pay zone exhibits $0.07 < \Phi t < 0.25$ (average value of 0.135 dec), $0.05 < \Phi e < 0.23$ (average value of 0.126 dec). Based on the higher

resistivity signature, the lower pay zone exhibits a lower average Sw of 0.167 and average BVW of 0.02. Pickett plot of both these zones from Sidri-9 indicates data cluster between Sw-25% and 50%, however majority of the data is around Sw 25% line (Fig. 13). This indicates excellent hydrocarbon potential in the Nukhul sandstone reservoirs.

Cross plot between bulk-density and neutron porosity in both the Sidri wells (Sidri-20 and Sidri-9) exhibits many data points lying close to the limestone line indicating the presence or influence of carbonates in the sandstones (Fig. 14). This behavior can be a result of calcareous cement or matrix in the Nukhul sandstones. The lithological observation matches with the cutting lithology description from the mud logs as well, which reports calcareous sandstones from the Nukhul interval in these Sidri wells. Based on the Potassium (K) and Thorium (Th) concentration from the spectral gamma ray data of the well Sidri-9, we infer montmorillonite to be the dominant clay phase in the studied Nukhul sandstone along with minor presence of kaolinite and illite (Fig. 15). A comparison of the inferred wireline log-based petrophysical properties in the three wells (ARS-6, Sidri-20, and two pay zones in Sideri-9) is presented in Fig. 16.
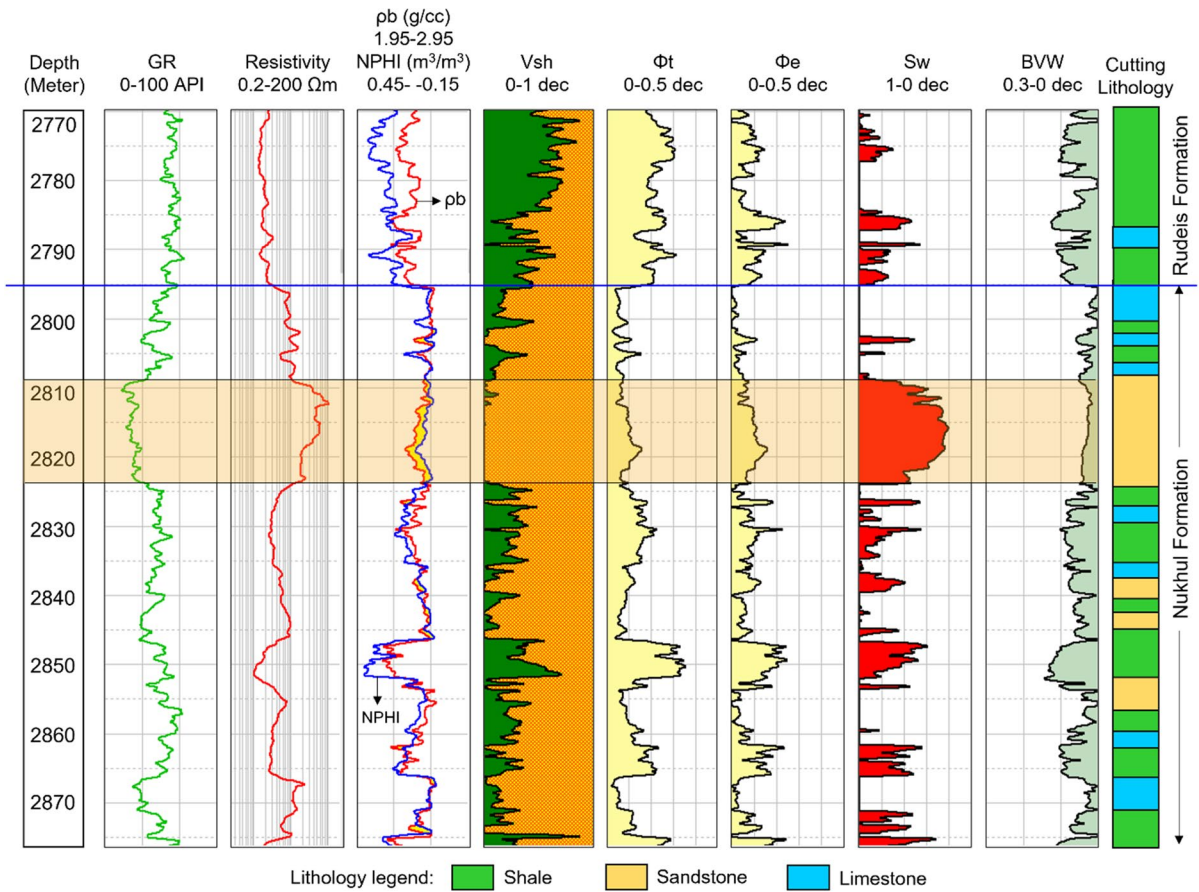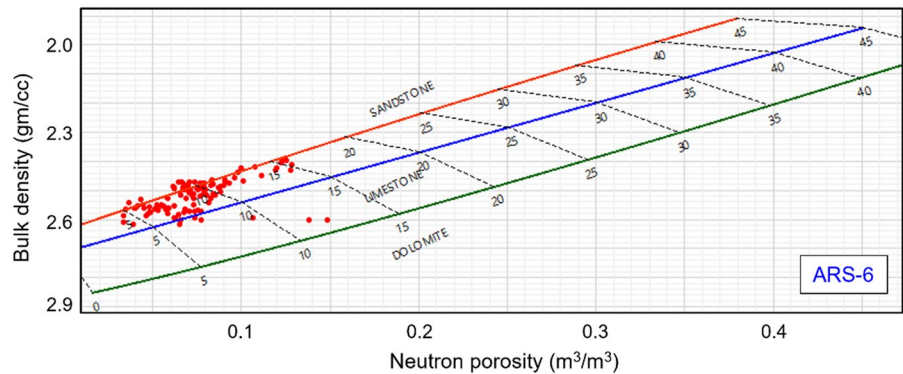
Fig. 7 Petrophysical analysis of the Nukhul Formation in the well ARS-6. The reservoir pay zone is highlighted by orange color

Fig. 8 Density-neutron porosity cross plot (Schlumberger 1972) exhibiting lithological distribution in the studied Nukhul reservoir zone from the well ARS-6

5 Discussions

The initial rifting phase between Upper Oligocene to Lower Miocene corresponds to the Abu Zenima conglomerate beds transitioning into fluvio-deltaic to marginal marine mixed carbonate-siliciclastic deposits of the Nukhul Formation (Patton et al. 1994). El Atfy et al. (2013) deciphered an algal and fungal proliferation within Nukhul interval which is indicative of shift from regressive environment to a transgressive one. Petrographic study was unavailable from the studied field; however literature survey

Fig. 9 Pickett plots to infer water saturation in the studied Nukhul Formation from the wells ARS-6 and Sidri-9
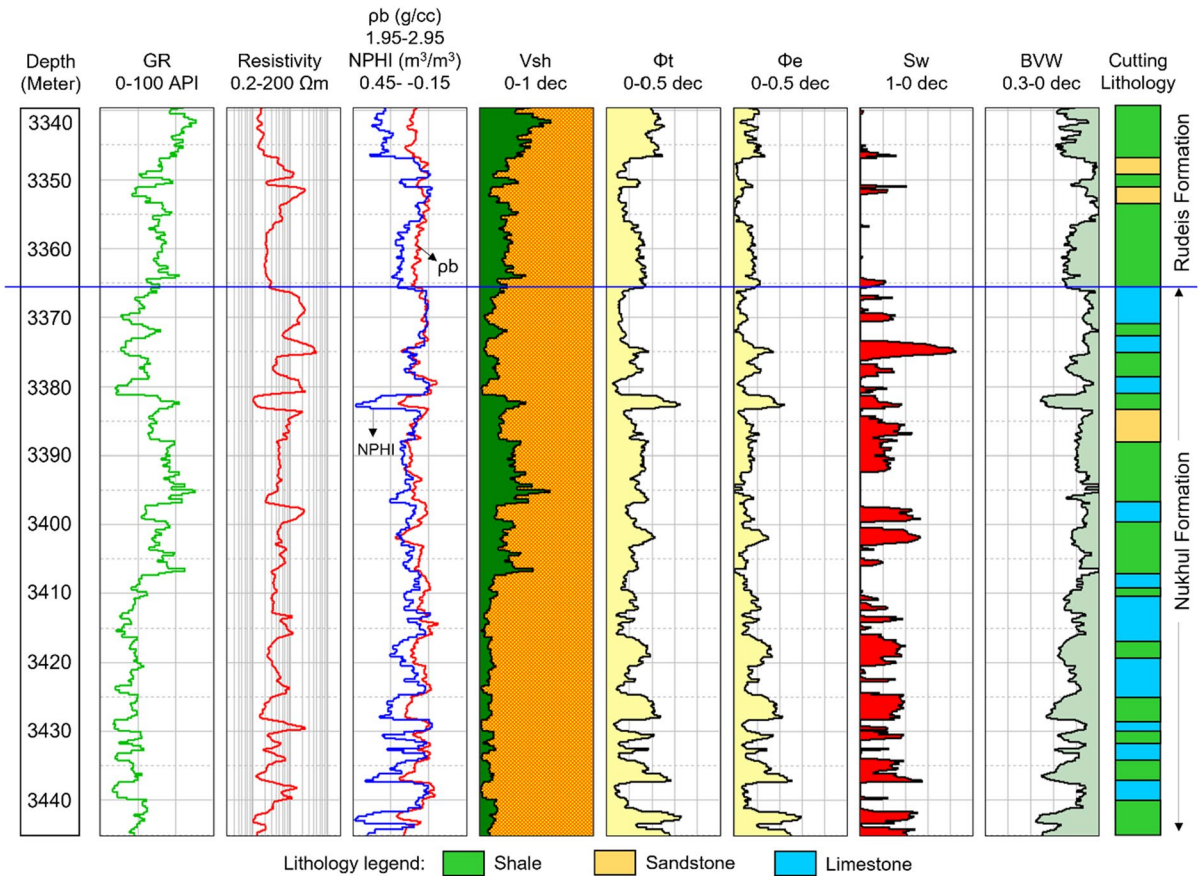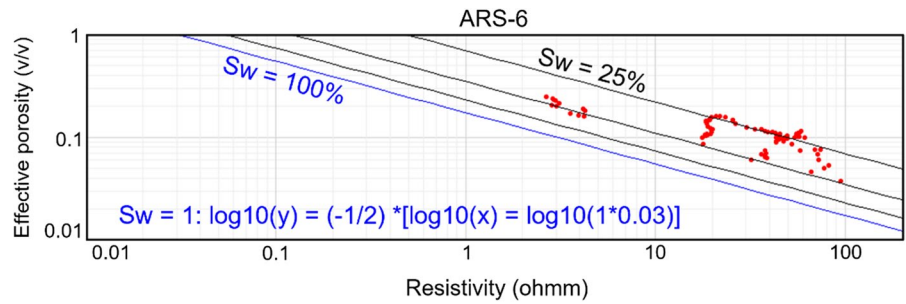

Fig. 10 Petrophysical analysis of the Nukhul Formation in the well ARM-7

provided critical insights. Winn et al. (2001) reported that the Nukhul sandstones consist of carbonate matrix. Zaid (2013) studied the petrographic characteristics of Nukhul clastics from West central Sinai and interpreted that the quartz arenites are cemented with ferran dolomite which also exhibited patchy dissolution contributing to the secondary porosity. El-Soughier and Mahmoud (2019) studied drill cutting samples from an offshore well GS9-1X drilled in the northern Gulf of Suez and inferred that the sandstones of the Nukhul interval are calcareous in nature, intercalated with slightly calcareous shale and crystalline hard limestone. El-Hafez et al. (2019) reported dolomite crystals from the SEM photographs of Nukhul sandstone samples from southwestern Sinai. Our observations from the density-neutron porosity also
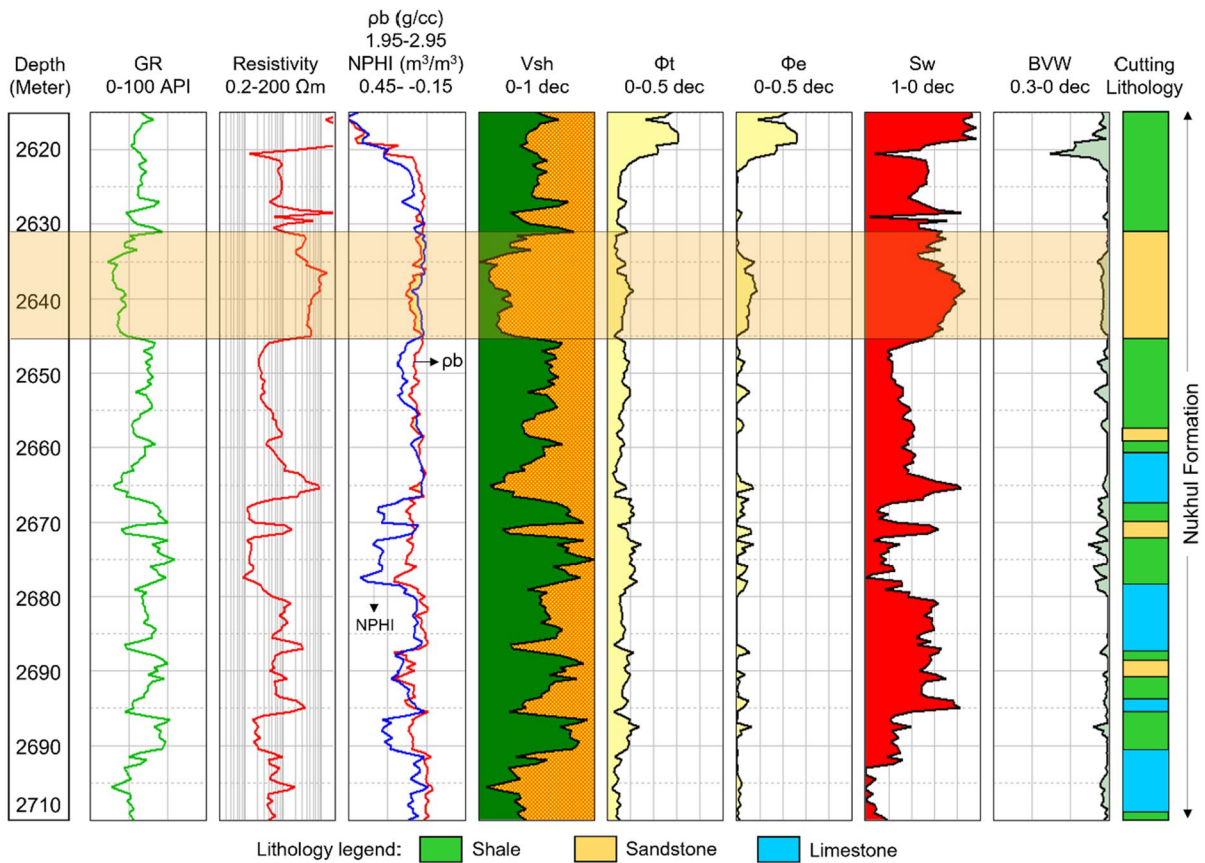
Fig. 11 Petrophysical analysis of the Nukhul Formation in the well Sidri-20. The reservoir pay zone is highlighted by orange color

corroborates with these reporting, as we observed many data points lying close to the limestone and dolomite lines indicating the presence or influence of carbonates in the sandstones, especially in the Sidri wells (Fig. 14). Spectral gamma ray data indicated dominance of montmorillonite along with minor kaolinite and illite within the Nukhul sandstones of the well Sidri-9 (Fig. 15). Similar observation was also made by El-Hafez et al. (2019) who reported montmorillonite and kaolinite as the principal clay phases based on the XRD and SEM results from southwestern Sinai area.

The seismic reflector corresponds to the Nukhul Formation in the Abu Rudeis-Sidri Field is discontinuous and intersected by several normal faults. Out of the four studied wells, ARM-7 was drilled in the hanging wall bounded by steeply dipping normal faults with a throw of more than 500 m. This well did not encounter any productive horizon,

which implies structural control on hydrocarbon accumulation. The evaluation of the hydrocarbon potential of the Nukhul Formation in the Abu Rudies-Sidri Field based on well log interpretation shows that this formation is a good oil reservoir, as also observed by Temraz and Dypvik (2018). According to Sarhan (2021), the Nukhul Formation has excellent petrophysical parameters in other fields too, particularly on the southern side of the Gulf of Suez (i.e., Rabeh East oil field), and its success depends on whether the drilled well penetrates a suitable structural closure. The identified productive reflector of Nukhul Formation has been correlated using well log data. The studied sandstone interval has good porosity values, hydrocarbon saturations, lower shale volume, and low water saturations, which are typical characteristics of a conventional productive clastic reservoir. Total porosity ranges between 7 and 16%. A similar porosity range
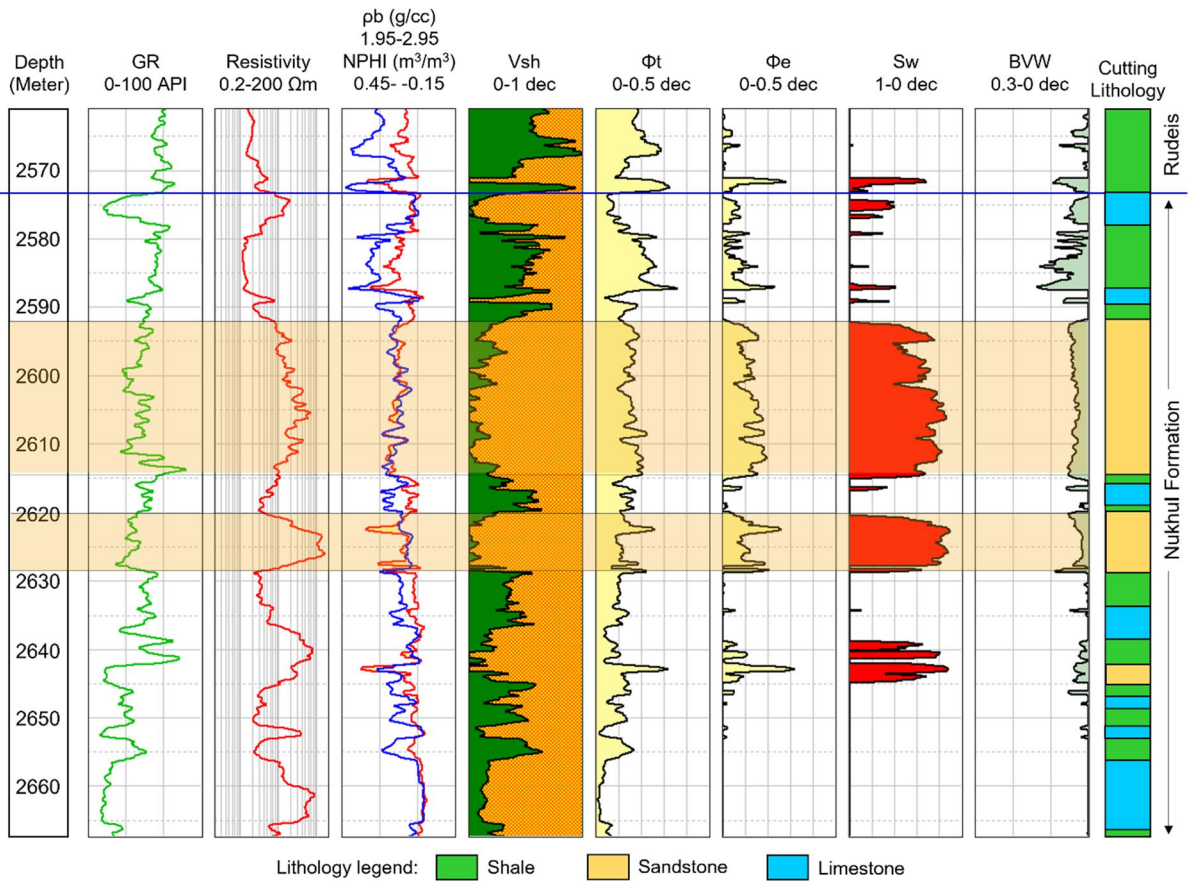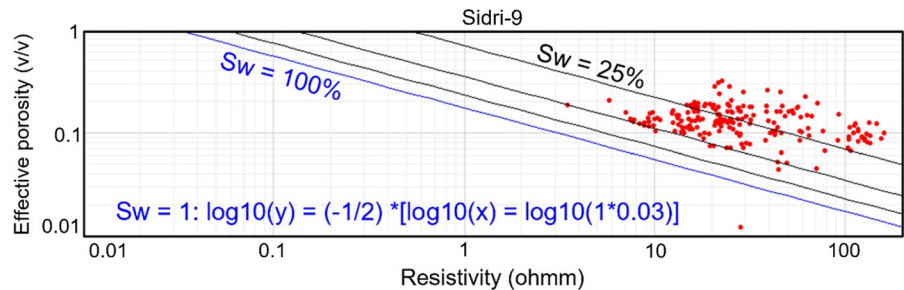
Fig. 12 Petrophysical analysis of the Nukhul Formation in the well Sidri-9. The reservoir pay zones are highlighted by orange color

Fig. 13 Pickett plots to infer water saturation in the studied Nukhul Formation from the wells ARS-6 and Sidri-9

was also reported by Abd El-Hafez et al. (2015) who inferred 3.8–19% porosity based on the routine core analysis of the Nukhul sandstones from southwestern Sinai. Inferred average porosity values in the Sidri-9 (~ 13.5–15.8%) are much higher than the Sidri-20 where Nukhul sandstone exhibits lowest porosities, i.e., 6.76%. This variation indicates higher lateral variability. These two wells also

exhibit high variability in the Vsh (sands in Sidri-9 are much cleaner). High lateral variability within Nukhul sandstones was also reported from the onshore Arta field, West Gharib concession in the Eastern Desert (Dongas and Crane 2021). The calculated water saturation of the reservoir zone in the three productive wells ranges between 17 and 34% (i.e., the hydrocarbon saturation equals 66–87%). A
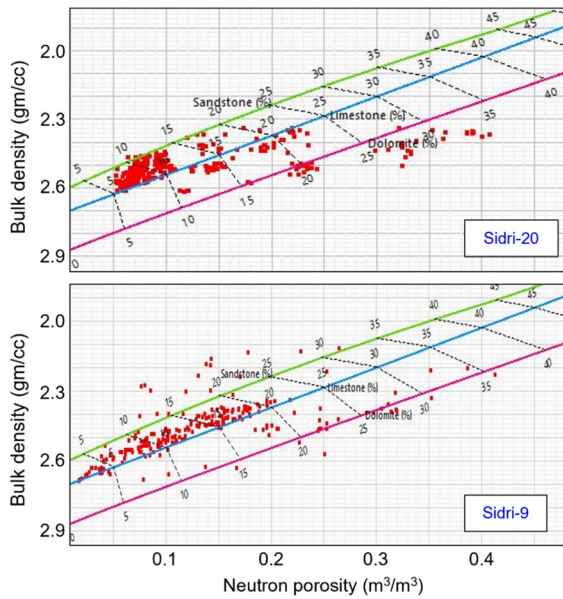
Fig. 14 Density-neutron porosity cross plot (Schlumberger 1972) exhibiting lithological distribution in the studied Nukhul reservoir zones from the wells Sidri-20 and Sidri-9
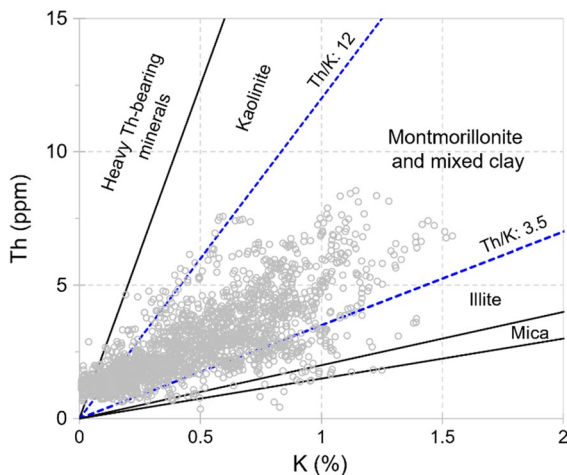

Fig. 15 Potassium–Thorium cross plot indicating montmorillonite as the dominant clay mineral within the Nukhul sandstone reservoir intervals in the well Sidri-9

small range of BVW indicates superior quality of the hydrocarbon-bearing sandstone intervals.

The petrophysical assessment presented in this study is based on the wireline logs. The inferred rock properties could not be calibrated with the direct core-based measurements, which possess as the

primary limitation. Unavailability of routine/special core analysis is a very common challenge in petrophysical evaluation projects, which has been the case for this study as well. Also clay mineralogy can be confirmed based on the X-ray diffraction (XRD) and scanning electron microscopy (SEM) dataset, which were unfortunately unavailable for this study.

6 Summary and conclusions

This study presents the key petrophysical properties of the oil-producing Nukhul sandstones in the Abu Rudeis-Sidri field. In absence of core-based measurements, this study utilized wireline logs to infer the reservoir characteristics. The conclusions of this study are as below:

- Nukhul sandstones exhibit ~10–16% total porosity with less than 34% water saturation indicating the excellent conventional reservoir quality.
- Lowest inferred Sw is around 17% from the Zone-2 in the well Sidri-9. BVW ranges between 0.011 and 0.036.
- Petrophysical cross plot indicates the calcareous nature of the Nukhul sandstones, with montmorillonite as dominant clay phase.
- Highest reservoir pay thickness is inferred in the well Sidri-9 where the reservoir is distributed in two zones, separated by a 5 m thick barrier.
- The Nukhul sandstones ARM-7 exhibit very high water saturation (~90%), therefore inferred unproductive.
- High lateral variability in shale volume and porosity distribution has been observed within the studied sandstones of nearby wells (i.e., Sidri-20 and Sidri-9).
- Preliminary seismic interpretation indicates steeply dipping normal faults with high throws. One of the studied wells in such deeper hanging wall did not encounter any productive zone indicating the critical structural implications for reservoir access across fault blocks.

A detailed structural interpretation (with 3D seismic dataset) clubbed with such reservoir petrophysical assessment will be immensely beneficial to understand the lateral variability and continuity of the Nukhul pay sands across the fault compartments

Fig. 16 Distribution of the estimated petrophysical parameters of the Nukhul reservoir intervals in the studied wells, Abu Rudeis—Sidri Field
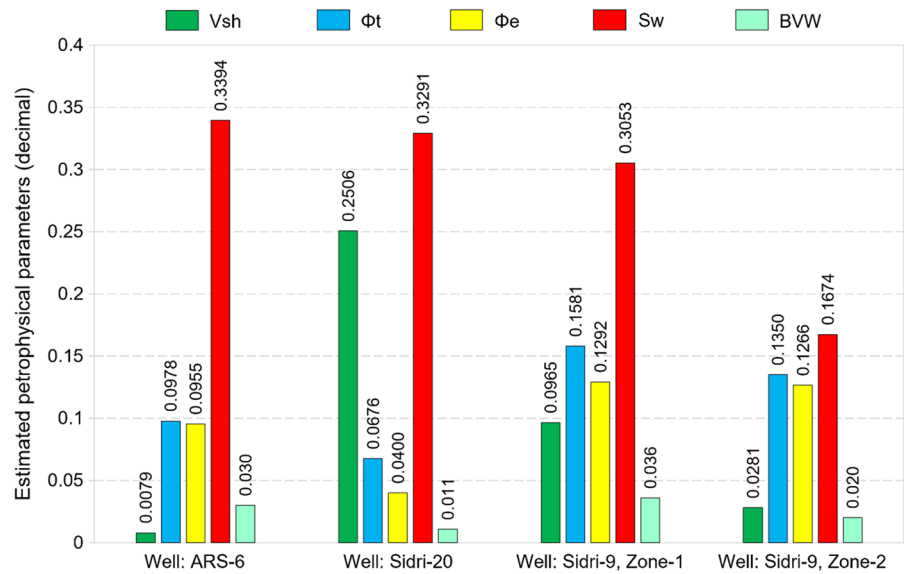
of the Abu Rudeis-Sidri field and contribute to identifying infill drilling locations for further field development.

Author contributions All authors have contributed equally in the data curation, project management, formal analysis, data interpretation, manuscript preparation and revision.

Data availability The geophysical data in the present work is confidential.

Declarations

Competing interests Here, we authorize that there is no conflict of interest.

Ethical approval We certify that this manuscript reflects our own research and has never been published before and not being considered for publication anywhere.

Consent to publish Here, we give our consent for the present manuscript to be published in this journal after the acceptance.

References

Abd El Gawad E, Abd El Hafez N, Hammed MS, El Naggar HA (2016) Characterization of pre-rift reservoirs of western Hurghada district, Egypt. Int J Innov Sci Eng Technol 3(12):74–83

Abd El-Gawad E, Fathy M, Mosad M, Refaat A, Metwally A (2022) Fracture recognition and characterization of the unconventional igneous intrusion reservoir in Rudeis-Sidri Field, Gulf of Suez, Egypt. J Geol Geophys 11(1):1102

Abd El-Hafez NA, Abd El-Moghny MW, Mousa AS, El-Hariri TY, Sharaka H (2015) Effect of diagenetic processes on storage capacity of Lower Miocene rocks at Southwestern Sinai, Egypt. Int J Sci Eng Appl Sci 1(9):176–197

Abd-Allah AM, Aal MHA, El-Said MM, El-Naby AA (2014) Structural evolution of the southern transfer zone of the Gulf of Suez rift. Egypt J Afr Earth Sci 96:21–38

Abul Karamat S, Meshref W (2002) Reverse fault geometry inthe Gulf of Suez Rift Basin, Egypt. In: International petroleum conference and exhibition, pp 27–30

Adelu AO, Aderemi AA, Akanji AO, Sanuade OA, Kaka SI, Afolabi O, Olugbemiga S, Oke R (2019) Application of 3D static modeling for optimal reservoir characterization. J Afr Earth Sci 152:184–196

Al-Husseini M (2012) Late oligocene–early miocene Nukhul Sequence, Gulf of Suez and Red Sea. Geoarabia 17:17–44

Alsharhan AS (2003) Petroleum geology and potential hydrocarbon plays in the Gulf of Suez rift basin, Egypt. AAPG Bull 87(1):143–180

Asquith G, Gibson C (1982) Basic well log analysis for geologists: methods in exploration series. AAPG, Tulsa

Awadalla A, Hegab OA, Ahmed MA, Hassan S (2018) Burial and thermal history simulation of the Abu Rudeis-Sidri oil field, Gulf of Suez-Egypt: a 1D basin modeling study. J Afr Earth Sci 138:86–101

Awadalla ASA, Farag AE, Hegab OA, Fadipe OA, Ahmed MA (2022) A multi-1D modeling and hydrocarbon expulsion assessment of a sulfur-rich Thebes-S organofacies, Abu Rudeis-Sidri oil field, Eastern Egypt. J Petrol Sci Eng 214:110500

Bosworth W, McClay KR (2001) Structural and stratigraphic evolution of the Gulf of Suez rift, Egypt: a synthesis. Mém Muséum Natl D'hist Nat 1993(186):567–606

Bosworth W, Huchon P, McClay K (2005) The red sea and gulf of aden basins. J Afr Earth Sci 43(1–3):334–378

Buckles RS (1965) Correlating and averaging connate water saturation data. J Can Pet Technol 4(1):42–52

Cheng B, Cheng S, Zhang G, Zhao D (2014) Seismic structure of the Helan–Liupan–Ordos western margin tectonic belt in North-Central China and its geodynamic implications. J Asian Earth Sci 87:141–156

Chowdhary LR, Taha S (1987) Geology and habitat of oil in Ras Budran field, Gulf of Suez, Egypt. AAPG Bull 71(10):1274–1293

Dongas JM, Crane G (2021) Unraveling the Nukhul reservoir in the Arta field, Egypt. In: Geoconvention, Virtual event, Sept 13–15

El Atfy H, Brocke R, Uhl D (2013) A fungal proliferation near the probable Oligocene/Miocene boundary, Nukhul Formation, Gulf of Suez, Egypt. J Micropalentol 32:183–195

El Diasty WS, El Beialy SY, Mostafa AR, Abo Ghonaim AA, Peters KE (2020) Chemometric differentiation of oil families and their potential source rocks in the Gulf of Suez. Nat Resour Res 29(3):2063–2102

El Nady MM, Ramadan FS, Hammad MM, Lotfy NM (2015) Evaluation of organic matters, hydrocarbon potential and thermal maturity of source rocks based on geochemical and statistical methods: case study of source rocks in Ras Gharib oilfield, central Gulf of Suez Egypt. Egypt J Pet 24(2):203–211

El-Hafez NA, Mousa A, El-Hariri T, El-Moghny MA, Sharaka H (2019) Mineralogical and geochemical studies on some early Miocene sediments of Southwestern Sinai, Egypt. Jordan J Earth Environ Sci 10(2):64–74

Elmaadawy KG, Bayan MF, El-Shayeb HM (2021) Source rock maturity and hydrocarbon potential of Abu Rudeis-Sidri area, central province, Gulf of Suez, Egypt. Arab J Geosci 14:2813

El-Soughier M, Mahmoud MS (2019) Dinoflagellate cysts stratigraphy and paleoecology from some Lower Miocene rocks, GS9-1X well, northern Gulf of Suez, Egypt. J Afr Earth Sci 160:103650

Fahmi A, El-Tokhy M, Attia A, Saber S, Madkour A (2015) Enhance oil recovery by discovering a new potential hydrocarbon from the unconventional reservoir, in Abu Rudeis/Sidri Field, Gulf of Suez Egypt. In: Offshore Mediterranean conference and exhibition, Ravenna, Italy, March, OMC, 290

Ghorab MA (1964) Oligocene and Miocene rock stratigraphy of the Gulf of Suez region. Egyptian General Petroleum Company, Start. Committee, Cairo, pp 1–142

Haque AKME, Qadri AMT, Bhuiyan MdAH, Navid M, Nabawy BS, Hakim MH, Abd-El-Aal AK (2022) Integrated wireline log and seismic attribute analysis for the reservoir evaluation: a case study of the Mount Messenger Formation in Kamiro Field, Taranaki Basin, New Zealand. J Nat Gas Sci Eng 99:104452

Islam MA, Yunsi M, Qadri SMT, Shalaby MR, Haque AKME (2021) Three-dimensional structural and petrophysical modeling for reservoir characterization of the Mangahewa Formation, Pohokura Gas-Condensate Field, Taranaki Basin, New Zealand. Nat Resour Res 30:371–394

Jenkins AP, Torvela T (2020) Basin analysis using seismic interpretation as a tool to examine the extent of a basin ore 'play.' Ore Geol Rev 125:103968

Kassem A, Sen S, Radwan AE, Abdelghany WK, Abioui M (2021) Effect of depletion and fluid injection in the Mesozoic and Paleozoic sandstone reservoirs of the October oil field, Central Gulf of Suez Basin: implications on drilling, production and reservoir stability. Nat Resour Res 30:2587–2606

Khan U, Zhang B, Du J, Jiang Z (2021) 3D structural modeling integrated with seismic attribute and petrophysical evaluation on hydrocarbon prospecting at the Dhulian oilfield, Pakistan. Front Earth Sci 5(3):649–675

Mostafa AR, Ganz H (1990) Source rock evaluation of a well in Abu Rudies area, Gulf of Suez. Berl Geowiss Abh 120:1002–1040

Mostafa AR, Klitzsch E, Matheis G, Ganz H (1993) Origin and evaluation of hydrocarbons in the Gulf of Suez basin. In: Thorweihe U, Schandelmaier H (eds) Geoscientific research in the North East Africa. Balkema, Rotterdam, pp 267–275

Moustafa AR, Khalil SM (2020) Structural setting and tectonic evolution of the Gulf of Suez, NW Red Sea and Gulf of Aqaba Rift Systems. The geology of Egypt. Springer, Cham, pp 295–342

NCGS (National Stratigraphic Subcommittee of the Geological Sciences of Egypt) (1974) Miocene rock stratigraphy of Egypt. Egypt J Geol 18(1):1–59

Omran MA (1995) Structural evolution of the central Gulf of Suez area from seismic data. Afr Geosci Rev 2(1):19–174

Patton TL, Moustafa AR, Nelson RA, Abdine SA (1994) Tectonic evolution and structural setting of the Suez rift. In: Landon SM (ed) Interior rift basins. American

Association of Petroleum Geologists Memoir, vol 59, pp 9–35

Peijs JA, Bevan TG, Piombino JT (2012) The Suez rift basin. In: Roberts DG, Bally AW (eds) Regional geology and tectonics: phanerozoic rift systems and sedimentary basins, vol 1B. Elsevier, Amsterdam, pp 165–194

Pickett GR (1972) Practical Fm evaluation. G.R. Pickett, Inc., Golden

Poupon A, Leveaux J (1971) Evaluation of water saturation in shaly formations. In: SPWLA 12th annual logging symposium. Society of petrophysicists and well-log analysts, Oklahoma, The Log Analyst, vol 12 (04)

Qadri SMT, Islam MA, Shalaby MR, Eashan ul Haque AKM (2017) Seismic interpretation and structural modeling of Kupe field, Taranaki Basin, New Zealand. Arab J Geosci 10:295

Qadri SMT, Islam MA, Shalaby MR (2019) Application of well log analysis to estimate the petrophysical parameters and evaluate the reservoir quality of the Lower Goru Formation, Lower Indus Basin, Pakistan. Geomech Geophys Geo-Energy Geo-Resour 5:271–288

Qadri SMT, Ahmed W, Haque AKME, Radwan AE, Hakimi MH, Abdel Aal AK (2022) Murree clay problems and water-based drilling mud optimization: a case study from the Kohat Basin in Northwestern Pakistan. Energies 15:3424

Radwan AE (2021a) Modeling pore pressure and fracture pressure using integrated well logging, drilling based interpretations and reservoir data in the giant El Morgan oil field, Gulf of Suez Egypt. J Afr Earth Sci 178:104165

Radwan AE (2021b) Modeling the depositional environment of the sandstone reservoir in the middle miocene sidri member, badri field, Gulf of Suez Basin, Egypt: integration of gamma-ray log patterns and petrographic characteristics of lithology. Nat Resour Res 30(1):431–449

Radwan AE, Sen S (2021a) Stress path analysis for characterization of in situ stress state and effect of reservoir depletion on present-day stress magnitudes: reservoir geomechanical modeling in the Gulf of Suez Rift Basin Egypt. Nat Resour Res 30(1):463–478

Radwan AE, Sen S (2021b) Characterization of in-situ stresses and its implications for production and reservoir stability in the depleted El Morgan hydrocarbon field, Gulf of Suez Rift Basin, Egypt. J Struct Geol 148:104355

Radwan AE, Kassem AA, Kassem A (2020) Radwany Formation: a new formation name for the early-middle eocene carbonate sediments of the offshore October oil field, Gulf of Suez: contribution to the Eocene sediments in Egypt. Mar Pet Geol 116:104304

Radwan AE, Abdelghany WK, Elkhawaga MA (2021a) Present-day insitu stresses in Southern Gulf of Suez, Egypt: insights for stress rotation in an extensional rift basin. J Struct Geol 147:104334

Radwan AE, Rohais S, Chiarella D (2021b) Combined stratigraphic structural play characterization in hydrocarbon exploration: a case study of Middle Miocene sandstones, Gulf of Suez basin, Egypt. J Asian Earth Sci 218:104686

Radwan AE, Trippetta F, Kassem AA, Kania M (2021c) Multi-scale characterization of unconventional tight carbonate reservoir: insights from October oil filed Gulf of Suez rift basin Egypt. J Pet Sci Eng 197:107968

Radwan AE, Sen S (2021c) Stress path analysis of the depleted Miocene clastic reservoirs in the El Morgan field, offshore Egypt. In: 55th U.S. rock mechanics/geomechanics symposium (ARMA), virtual, June 18–25. ARMA-2021c-1346

Radwan AE, Sen S (2021d) Stress path analysis of the depleted Middle Miocene clastic reservoirs in the Badri field, Gulf of Suez Rift Basin, Egypt. In: SPE annual technical conference and exhibition (ATCE), Dubai, UAE, Sept 21–23: SPE-205900

Saoudi A, Khalil B (1986) Distribution and hydrocarbon potential of Nukhul sediments in the Gulf of Suez. In: Proceedings of the 7th exploration seminar, Cairo, 1984, Egyptian General Petroleum Corporation, Cairo, Egypt, pp 75–96

Sarhan MA (2021) Geophysical and hydrocarbon prospect evaluation of Nukhul Formation at Rabeh East oil field, Southern Gulf of Suez Basin, Egypt. J Pet Explor Prod Technol 11(7):2877–2890

Schlumberger (1972) Log interpretation/charts. Schlumberger Well Services Inc, Houston

Schlumberger (1995) Well evaluation conference, Egypt. Paris, France, p 87

Schutz KI (1994) Structure and stratigraphy of the Gulf of Suez, Egypt: chapter 2: part I. Type Basin: Gulf of Suez, pp 57–96

Sultan N (2002) Gulf of Suez/Red sea structural evaluation and hydrocarbon potentiality. In: International petroleum conference and exhibit, p 82

Temraz M, Dypvik H (2018) The lower Miocene Nukhul Formation (Gulf of Suez, Egypt): microfacies and reservoir characteristics. J Petrol Explor Prod Technol 8(1):85–98

Waite ST, Pooley RW (1953) Report on the Nukhul Formation. Unpublished report GR Egyptian General Petroleum Co-operation, Egypt, 952 pp

Winn RD Jr, Crevello PD, Bosworth W (2001) Lower Miocene Nukhul Formation, Gebel el Zeit, Egypt: model for structural control on early synrift strata and reservoirs Gulf of Suez. AAPG Bull 85(10):1871–1890

Youssef A (2011) Early-middle Miocene Suez syn-rift-basin, Egypt: a sequence stratigraphy framework. GeoArabia 16(1):113–134

Zahra HS, Nakhla A (2016a) Tectonic and structural setting of the northeastern Gulf of Suez area using aeromagnetic data. J Afr Earth Sci 115:1–16

Zahra HS, Nakhla AM (2016b) Structural interpretation of seismic data of Abu Rudeis-Sidri area, northern Central Gulf of Suez, Egypt. NRIAG J Astron Geophys 5(2):435–450

Zaid SM (2013) Genesis of the Nukhul sandstones, west central Sinai, Egypt. J Appl Sci Res 9(1):375–392

Zhang B, Tong Y, Du J, Hussain S, Jiang Z, Ali S, Ali I, Khan M, Khan U (2022) Three-dimensional structural modeling (3D SM) and joint geophysical characterization (JGC) of hydrocarbon reservoir. Minerals 12:363